

# Femtosecond X-ray measurement of coherent lattice vibrations near the Lindemann stability limit

Klaus Sokolowski-Tinten\*, Christian Blome\*, Juris Blums\*, Andrea Cavalleri†, Clemens Dietrich\*, Alexander Tarasevitch\*, Ingo Uschmann‡, Eckhard Förster‡, Martin Kammler§, Michael Horn-von-Hoegen\* & Dietrich von der Linde\*

\* Institut für Laser- und Plasmaphysik, Universität Essen, 45117 Essen, Germany

† Materials Science Division, Lawrence Berkeley National Laboratory, Berkeley, California 94720, USA

‡ Forschungsgruppe Röntgenoptik, Institut für Optik und Quantenelektronik, Friedrich-Schiller-Universität Jena, 07743 Jena, Germany

§ Institut für Halbleitertechnologie, Universität Hannover, 30167 Hannover, Germany

The study of phase-transition dynamics in solids beyond a time-averaged kinetic description requires direct measurement of the changes in the atomic configuration along the physical pathways leading to the new phase. The timescale of interest is in the range  $10^{-14}$  to  $10^{-12}$  s. Until recently, only optical techniques were capable of providing adequate time resolution<sup>1</sup>, albeit with indirect sensitivity to structural arrangement. Ultrafast laser-induced changes of long-range order have recently been directly established for some materials using time-resolved X-ray diffraction<sup>2–8</sup>. However, the measurement of the atomic displacements within the unit cell, as well as their relationship with the stability limit of a structural phase<sup>9–11</sup>, has to date remained obscure. Here we report time-resolved X-ray diffraction measurements of the coherent atomic displacement of the lattice atoms in photoexcited bismuth close to a phase transition. Excitation of large-amplitude coherent optical phonons gives rise to a periodic modulation of the X-ray diffraction efficiency. Stronger excitation corresponding to atomic displacements exceeding 10 per cent of the nearest-neighbour distance—near the Lindemann limit—leads to a subsequent loss of long-range order, which is most probably due to melting of the material.

The most common crystalline form of bismuth is the  $\alpha$ -arsenic or

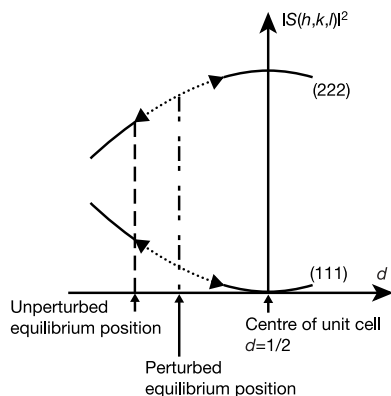


**Figure 1** Geometrical structure factor  $|S(h, k, l)|^2$  of bismuth as a function of the distance  $d$  of the two basis atoms for diffraction from (111) and (222) lattice planes. The dotted lines denote the atomic movement after an impulsive shift of the equilibrium Bi–Bi distance upon transition to an excited electronic state.

A7 structure<sup>12</sup>. The lattice can be derived from the face-centred-cubic lattice by a weak rhombohedral distortion of the cubic unit cell. The crystal basis consists of two Bi atoms: atom 1 on a lattice site, and atom 2 at a position slightly displaced from the centre along the body diagonal of the unit cell.

The distortion from the cubic structure to A7 is stabilized by the so-called Peierls–Jones<sup>13</sup> mechanism, which introduces a small bandgap over extended regions of the Brillouin zone and is responsible for bismuth being a semimetal. However, the equilibrium structure, particularly the equilibrium distance of the two basis atoms, can be easily perturbed by external influences—for example, by changes of pressure and temperature, or by electronic excitation<sup>14,15</sup>. When the distance is changed by a fast perturbation, the Bi atoms perform a damped oscillation along the body diagonal and finally come to rest at the new equilibrium position. This mode of coherent atomic motion represents a totally symmetric  $A_{1g}$  optical phonon mode of the crystal.

Excitation of coherent lattice vibrations by an impulsive perturbation of the atomic equilibrium position (displacive excitation) has previously been studied in a variety of materials<sup>15–20</sup>, including bismuth. In these experiments femtosecond laser excitation was used, and the atomic motion was detected indirectly by measuring the weak oscillations in the optical reflectivity at the phonon frequency that are produced by the lattice vibrations.

A direct way of observing the evolution of the atomic configuration is to use time-resolved X-ray diffraction. The changes in the diffraction efficiency caused by atomic motion in the unit cell are determined by the squared modulus of the geometrical structure factor  $|S(h, k, l)|^2$ , where  $h, k$  and  $l$  are Miller indices. Figure 1 compares the X-ray diffraction from lattice planes of bismuth corresponding to  $(hkl) = (111)$  and  $(hkl) = (222)$ .  $|S|^2$  is plotted as a function of the Bi–Bi distance  $d$  (in units of the length of the body diagonal). For  $d = 1/2$  (atom 2 in the centre), diffraction from (111) planes is forbidden, whereas (222) diffraction has a maximum. The actual equilibrium value of  $d$  in the unperturbed crystal is marked by the dashed vertical line ( $d = 0.468$ ).

We now consider a perturbation that sets the atoms in motion towards a new equilibrium position with atom 2 closer to the centre of the unit cell (dash-dotted line in Fig. 1). As this motion proceeds, we expect to see changes in the X-ray diffraction signal in opposite directions: an increase for (222) and a decrease for (111). Following these initial changes, the oscillatory atomic motion should give rise to oscillations both in the (222) and the (111) X-ray diffraction with a frequency corresponding to the  $A_{1g}$  optical phonon mode.

In the time-resolved X-ray diffraction experiments reported here,

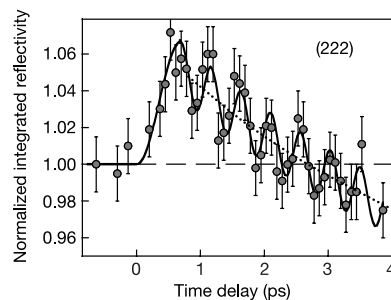


**Figure 2** X-ray diffraction efficiency of the (222) reflection as a function of time delay between the optical pump pulse (fluence  $6 \text{ mJ cm}^{-2}$ ) and the X-ray probe pulse. The solid line is fitted to the experimental data. The decrease of the mean value of the X-ray signal (dotted line) is explained by the Debye–Waller effect, and reflects the increasing random component of the atomic motion.

## letters to nature

we studied crystalline bismuth films of 50 nm thickness and (111) surface orientation. X-ray pulses at a photon energy of 4.51 keV (wavelength 0.274 nm) were used. The material was optically excited by near-infrared (800 nm) femtosecond laser pulses with an energy fluence of  $6 \text{ mJ cm}^{-2}$  in order to launch a strong  $A_{1g}$  optical phonon mode through displacive excitation. The atomic motion underlying the excited lattice wave was probed by measuring the diffraction of the X-ray probe pulses interacting with the lattice after a controlled time delay with respect to the laser pulses. Measurements were performed at two different Bragg angles,  $\theta_{111} = 20^\circ$  and  $\theta_{222} = 44^\circ$ , in order to compare the X-ray diffraction from (111) and (222) lattice planes.

The result of the (222) experiment is shown in Fig. 2. The measured X-ray diffraction signal (integrated reflectivity) is plotted as a function of the time delay between the laser pulses and the X-ray pulses. As the time is increased, an initial increase in the diffraction signal within a few hundred femtoseconds is observed. The first maximum of the diffraction signal is followed by a sequence of distinct periodic minima and maxima. This feature of the data clearly indicates oscillations in the temporal evolution of the X-ray diffraction efficiency. The solid curve in Fig. 2 is a fit to the experimental data. The oscillatory part of the fit consists of constant cycles of 467 fs, corresponding to a frequency  $\nu = 2.12 \text{ THz}$ . No effort has been made to take into account damping or changes in the cycle duration.

We performed similar measurements for a crystal orientation in which the diffraction from (111) lattice planes could be recorded. In this case an initial decrease in the diffraction is observed, followed by a series of maxima and minima very similar to what was measured in the (222) diffraction experiment, but in the opposite sense (Fig. 3). The period of these oscillations agrees with the oscillation frequency  $\nu = 2.12 \text{ THz}$  observed in the (222) experiment. (The data point at the far right in Fig. 3 represents diffraction measurements taken several seconds after the laser excitation pulse. A full recovery of the crystal diffraction is observed, indicating that no laser damage or other material modifications have occurred.)

From the measured changes in the X-ray diffraction, the actual atomic displacement can be obtained. If it is assumed that the variation of the X-ray signal is dominated by changes in  $d$ , the initial increase of 7% in the (222) diffraction corresponds to a  $\Delta d$  of approximately 0.015–0.025 nm. The two principal sources of error in  $\Delta d$ , besides the experimental error bars, are uncertainties concerning the depth profile of the excited Bi layer and the smoothing of the oscillations caused by the finite duration of the X-ray probe pulses. Linear absorption data of Bi correspond to a penetration depth of 14–22 nm (ref. 12), suggesting that only a fraction of the 50-nm Bi film is optically excited and contributes

to changes in the X-ray diffraction signal. From independent experiments we have obtained a value of about 300 fs for the width of the X-ray pulses<sup>21</sup>. Deconvolution calculations using this pulse width imply that the actual oscillation amplitudes are approximately twice as large as the observed oscillations of the X-ray signal.

A comparison of the observed frequency  $\nu = 2.12 \text{ THz}$  with the  $A_{1g}$  optical phonon frequency of the unperturbed bismuth crystal ( $\nu_{1g} = 2.92 \text{ THz}$ ) indicated that the phonon frequency is significantly downshifted in the highly excited material. Very recently, frequency downshifts to 2.45 THz were observed by Hase *et al.*<sup>20</sup> in displacive excitation experiments in which the coherent phonons were detected through changes in the optical reflectivity. The frequency shifts were found to be dependent on the phonon oscillation amplitude, and the effect was attributed to anharmonicity<sup>21</sup>. Here, we observe a much larger downshift. The measured maximum atomic displacements correspond to a significant fraction of the nearest-neighbour distance ( $d_{nn} = 0.31 \text{ nm}$ ) of the Bi atoms in the A7 structure,  $\Delta d/d_{nn} \approx 5\text{--}8\%$ . Such large atomic displacements are expected to lead to important changes in the crystal potential, and eventually to a destabilization of the crystal structure and structural phase transitions. The Lindemann criterion<sup>8</sup> states that the solid-to-liquid phase transition occurs when the mean displacement of the lattice atoms reaches 10–20% of the lattice constant.

Indeed, we observed structural disordering of bismuth when the laser excitation was further increased. An example is depicted in Fig. 4, which shows the integrated X-ray reflectivity of the (222) diffraction as a function of pump–probe time delay for an excitation fluence of  $20 \text{ mJ cm}^{-2}$ . At this excitation level, an initial increase in the diffraction signal as large as 20% within a few hundred femtoseconds was observed. Subject to the uncertainties described above, we conclude that this strong change in the diffraction signal corresponds to an initial coherent atomic displacement of nearly 0.04 nm, or more than 10% of the nearest-neighbour distance.

However, in clear contrast to the observations at lower excitation, no oscillations of the diffraction signal occurred. Instead, it was observed that after reaching the maximum the diffraction signal decreased monotonically, and reached a quasi-stationary level of 40% in approximately 10 ps. We interpret this decrease as an indication of disordering due to melting of the material. This explanation is supported by the observed shift of the Bragg peak towards smaller diffraction angles. The shifts can be attributed to thermal expansion, and indicate that the temperature of the non-disordered material underneath the disordered surface layer is close to the melting point of bismuth. Diffraction data on the (111) reflection are in line with this interpretation.

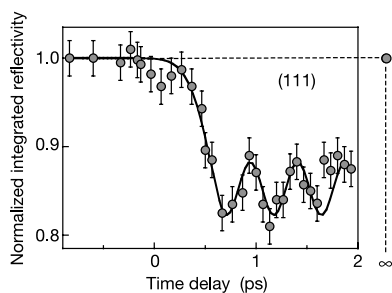


**Figure 3** X-ray diffraction efficiency of the (111) reflection as a function of time delay between the optical pump pulse (fluence  $6 \text{ mJ cm}^{-2}$ ) and the X-ray probe pulse. The solid line is fitted to the experimental data. The Debye–Waller effect in (111) diffraction is negligible.

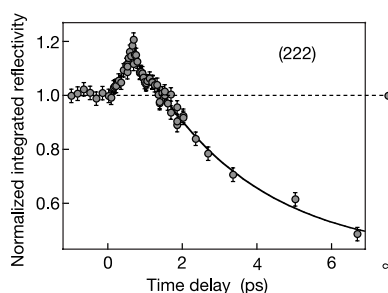


**Figure 4** X-ray diffraction efficiency of the (222) reflection as a function of time delay between the optical pump pulse (fluence  $20 \text{ mJ cm}^{-2}$ ) and the X-ray probe pulse.

We believe that the present study represents a significant step beyond the observation of long-range order loss that was made in previous X-ray experiments on ultrafast non-thermal melting: in these previous experiments, it was not possible to obtain the initial displacements. Although the relationship between the large coherent displacements of the lattice atoms observed in the present work and the stability of the parent phase is still elusive, our experiments establish a direction for future studies—the use of X-ray scattering on the appropriate timescale to reveal details of product phase formation. □

**Methods**

The X-ray pulses were generated by focusing femtosecond laser pulses from a titanium:sapphire laser system (120-fs pulse width, about 100-mJ pulse energy, 10-Hz repetition rate) onto a thin titanium wire to produce a microplasma<sup>21</sup>. The incoherent X-ray emission from the laser-produced plasma (Ti K $\alpha$  line at 0.274 nm) was collected, and focused onto a spot of approximately 80  $\mu$ m in the centre of the laser-excited area on the surface of the bismuth crystal. To focus the X-rays, we used a toroidally bent silicon crystal. The 50-nm Bi films were grown heteroepitaxially on a Si(111) wafer. The growth process provided high-quality single crystalline layers of bismuth with a lattice constant different from that of the Si substrate. This allows us to isolate the relatively weak X-ray diffraction of the thin Bi film from the strong background diffraction due to the Si substrate. An X-ray-sensitive electronic camera was used to record the angular distribution of the diffracted X-rays. The X-ray signal integrated over the diffraction angle (integrated reflectivity) typically corresponded to 10 diffracted photons per pulse. Therefore, signal integration over many thousands of pulses was necessary to achieve a measuring accuracy of several per cent.

Received 7 October 2002; accepted 7 February 2003; doi:10.1038/nature01490.

1. Bloembergen, N. From nanosecond to femtosecond science. *Rev. Mod. Phys.* **71**, S283–S287 (1999).
2. Chin, A. H. *et al.* Ultrafast structural dynamics in InSb probed by time-resolved X-ray diffraction. *Phys. Rev. Lett.* **83**, 336–339 (1999).
3. Siders, C. W. *et al.* Detection of non-thermal melting by ultrafast X-ray diffraction. *Science* **286**, 1340–1342 (1999).
4. Lindenberg, A. M. *et al.* Time-resolved X-ray diffraction from coherent phonons during a laser-induced phase transition. *Phys. Rev. Lett.* **84**, 111–114 (2000).
5. Rouse, A. *et al.* Non-thermal melting in semiconductors measured at femtosecond resolution. *Nature* **410**, 65–68 (2001).
6. Sokolowski-Tinten, K. *et al.* Femtosecond X-ray measurement of ultrafast melting and large acoustic transients. *Phys. Rev. Lett.* **87**, 225701 (2001).
7. Cavalleri, A. *et al.* Femtosecond structural dynamics in VO<sub>2</sub> during an ultrafast solid-solid phase transition. *Phys. Rev. Lett.* **87**, 237401 (2001).
8. Feurer, T. *et al.* Femtosecond silicon K $\alpha$  pulses from laser produced plasmas. *Phys. Rev. E* **65**, 016412 (2002).
9. Lindemann, F. A. Über die Berechnung molekularer Eigenfrequenzen. *Phys. Z.* **11**, 609–612 (1910).
10. Born, M. Thermodynamics of crystals and melting. *J. Chem. Phys.* **7**, 591–603 (1939).
11. Tallon, J. L. A hierarchy of catastrophes as a succession of stability limits for the crystalline state. *Nature* **342**, 658–660 (1989).
12. Madelung, O. (ed.) *Semiconductors: Physics of Non-tetrahedrally Bonded Elements and Binary Compounds I* in Landolt-Börnstein, New Series, Group III: *Crystal and Solid State Physics* Vol. 17, *Semiconductors*, Part a (Springer, Berlin, 1983).
13. Peierls, R. *More Surprises in Theoretical Physics* (Princeton Univ. Press, Princeton, 1991).
14. Shick, A. B., Ketterson, J. B., Novikov, D. L. & Freeman, A. J. Electronic structure, phase stability, and semimetal-semiconductor transitions in Bi. *Phys. Rev. B* **60**, 15484–15487 (1999).
15. Zeiger, H. J. *et al.* Theory for dispersive excitation of coherent phonons. *Phys. Rev. B* **45**, 768–778 (1992).
16. Hunsche, S., Wienecke, K., Dekorsy, T. & Kurz, H. Impulsive softening of coherent phonons in tellurium. *Phys. Rev. Lett.* **75**, 1815–1818 (1995).
17. Garrett, G. A., Albrecht, T. E., Whitaker, J. F. & Merlin, R. Coherent THz phonons driven by light pulses and the Sb problem: what is the mechanism? *Phys. Rev. Lett.* **77**, 3661–3664 (1996).
18. Hase, M., Mizoguchi, K., Harima, H. & Nakashima, S. Dynamics of coherent phonons in bismuth generated by ultrashort light pulses. *Phys. Rev. B* **58**, 5448–5452 (1998).
19. DeCamp, M. F., Reis, D. A., Bucksbaum, P. H. & Merlin, R. Dynamics and coherent control of high-amplitude phonons in bismuth. *Phys. Rev. B* **64**, 092301 (2001).
20. Hase, M., Kitajima, M., Nakashima, S. & Mizoguchi, K. Dynamics of coherent anharmonic phonons in bismuth using high density photoexcitation. *Phys. Rev. Lett.* **88**, 067401 (2002).
21. Von der Linde, D. *et al.* 'Ultrafast' extended to X-rays: Femtosecond time-resolved X-ray diffraction. *Z. Phys. Chem.* **215**, 1527–1541 (2001).

**Acknowledgements** Financial support by the Deutsche Forschungsgemeinschaft, the European Community (Research and Training Network XPOSE) and the German Academic Exchange Service (DAAD) is acknowledged.

**Competing interests statement** The authors declare that they have no competing financial interests.

**Correspondence** and requests for materials should be addressed to K.S.-T. (e-mail: kst@ilp.physik.uni-essen.de).

**Phonon interpretation of the 'boson peak' in supercooled liquids**

T. S. Grigera\*†, V. Martin-Mayor\*†, G. Parisi\* & P. Verrocchio†‡

\* Dipartimento di Fisica, Sezione INFN, SMC and INFN unità di Roma 1, Università di Roma "La Sapienza", Piazzale Aldo Moro 2, I-00185 Roma, Italy  
 † Dipartimento di Fisica and INFN unità di Trento, Università di Trento, Via Sommarive, 14, 38050 Povo, Trento, Italy

Glasses<sup>1,2</sup> are amorphous solids, in the sense that they display elastic behaviour. In crystalline solids, elasticity is associated with phonons, which are quantized vibrational excitations. Phonon-like excitations also exist in glasses at very high (terahertz; 10<sup>12</sup> Hz) frequencies; surprisingly, these persist in the supercooled liquids<sup>3</sup>. A universal feature of such amorphous systems is the boson peak: the vibrational density of states has an excess compared to the Debye squared-frequency law. Here we investigate the origin of this feature by studying the spectra of inherent structures<sup>4</sup> (local minima of the potential energy) in a realistic glass model. We claim that the peak is the signature of a phase transition in the space of the stationary points of the energy, from a minima-dominated phase (with phonons) at low energy to a saddle-point-dominated phase<sup>5–7</sup> (without phonons). The boson peak moves to lower frequencies on approaching the phonon–saddle transition, and its height diverges at the critical point. Our numerical results agree with the predictions of euclidean random matrix theory<sup>8</sup> on the existence of a sharp phase transition<sup>9</sup> between an amorphous elastic phase and a phonon-free one.

Vibrational excitations of glasses in the terahertz region, and the related vibrational density of states (VDOS), are important in their thermodynamic properties<sup>10</sup>. Recent results suggest that the VDOS is determined by the properties of the potential energy landscape<sup>4</sup> (PEL), a tool useful in the understanding of the slow dynamics of supercooled liquids<sup>2</sup>. Indeed, the VDOS and the dynamic structure factor can be qualitatively reproduced from the (harmonic) vibrational spectrum obtained from the diagonalization of the hessian matrix of the potential energy evaluated at the minima ('inherent structures') of a Lennard–Jones system<sup>11</sup>. The same numerical procedure has led to quantitative agreement with inelastic X-ray scattering experiments in amorphous silica<sup>12</sup>. Here we will show that a boson peak must be present in the VDOS as a consequence of the PEL geometry; we also make quantitative predictions, which can be checked by rapidly quenching supercooled liquids below their glass temperature.

The high-frequency (0.1–10 THz) excitations have been experimentally shown to have linear dispersion relations<sup>3,13–18</sup> in the mesoscopic momentum region (~1–10 nm<sup>-1</sup>). Although clearly not plane waves, they are highly reminiscent of phonons, both because they propagate with the speed of sound, and because the VDOS  $g(\omega)$  ( $\omega$  is the frequency) is Debye-like ( $g(\omega) \propto \omega^2$ ) at low enough frequency. These excitations have in fact been dubbed 'high-frequency sound', and a coherent theoretical picture of their properties has been obtained<sup>9,19,20</sup> using euclidean random matrix theory<sup>8</sup> (ERMT).

However, there is more to the low-frequency VDOS of glasses than the Debye law. A characteristic feature is that the VDOS departs from the Debye form, displaying an excess of states, which has been named the boson peak. As observed in many materials<sup>3,13–18</sup>, the boson peak is in a region of frequencies where

† Present addresses: Centro di Studi e Ricerche "Enrico Fermi", via Panisperna, 89/A, 00184 Roma, Italy (T.S.G.); Departamento de Física Teórica I, Universidad Complutense de Madrid, Avenida Complutense, 28040 Madrid, Spain (V.M.-M., P.V.).